

# Multi-Robot Trajectory Planning with Feasibility Guarantee and Deadlock Resolution: An Obstacle-Dense Environment

Yuda Chen, Chenghan Wang, and Zhongkui Li

**Abstract**—This article presents a multi-robot trajectory planning method which guarantees optimization feasibility and resolves deadlocks in an obstacle-dense environment. The method is proposed via formulating an optimization problem, where the modified buffered Voronoi cell with warning band is utilized to avoid the inter-robot collision and the deadlock is resolved by an adaptive right-hand rule. Meanwhile, a novel safe corridor derived from historical planned trajectory is proposed to provide a proper space for obstacle avoidance in trajectory planning. Comparisons with state-of-the-art works are conducted to illustrate the safety and deadlock resolution in cluttered scenarios. Additionally, hardware experiments are carried out to verify the performance of the proposed method where eight nano-quadrotors fly through a 0.6m cubic framework.

**Index Terms**—Trajectory generation, motion planning, multi-robot system, collision avoidance, deadlock resolution.

## I. INTRODUCTION

**C**OLLISION-free trajectory planning plays an essential role in the missions preformed by a swarm of robots in a shared environment, such as cooperative inspection and transportation [1], [2]. Currently, optimization-based methods, such as model predictive control [3] and sequential convex program [4], are widely employed to handle collision avoidance by introducing different kinds of constraints. However, the constrained optimization problem may suffer from infeasibility leading to the failure of replanning, and such a phenomenon occurs more frequently in a crowded environment. Furthermore, in obstacle-dense situations, the robots in the swarm are more likely to get stuck with each other, which is also known as deadlock [5].

Concerning the multi-robot trajectory planning problem in an obstacle-dense environment, we propose a novel method to ensure the optimization feasibility and handle the deadlock problem simultaneously. In this work, the modified buffered Voronoi cell with warning band (MBVC-WB) [6] is utilized to deal with inter-robot collision avoidance, and the assorted adaptive right hand rule is brought in for deadlock resolution. Furthermore, in order to avoid obstacles in the environment, a safe corridor is generated to provide a feasible space for trajectory replanning. Specifically, we firstly adopt a search-based path planning method ABIT\* [7] to determine an approximated path in the complex environment. Then, the

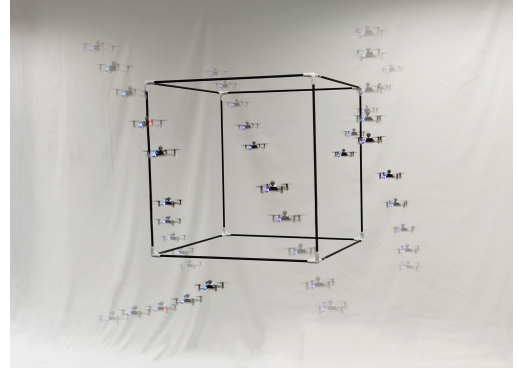


Fig. 1. Eight nano-quadrotors fly through a cubic framework.

separating hyperplane is constructed between the imminent obstacles and the existing planned trajectory based on a quadratic program.

The main contributions of this work are summarized as follows.

- A novel safe corridor constituted by a sequence of polyhedron is proposed for obstacle avoidance, and it is formed via an online method, different from those offline ones as in [8], [9]. In contrast to the rectangular safe corridor in [10], [11], [12], the presented corridor provides a more reasonable planning space by considering the motion tendency of robots and the distribution of obstacles in the environment.
- Different from [6] where the deadlock resolution is performed in a free space, this work considers an obstacle-dense environment, which is evidently more challenging. In addition, the penalty term related to the warning band is replaced by a quadratic one which considerably mitigates the computation time.
- Comparisons with state-of-the-art results [11], [13], [14] are made in several cluttered scenarios, illustrating that the proposed method has a better performance in terms of guaranteeing the collision avoidance as well as handling the deadlock problem.
- Hardware experiments are executed to verify the validation in real-world cases, including eight crazyfiles passing through a 3D framework (Fig. 1), four crazyfiles transitting in a polygonal environment, and six and eight robots going through “H”-and “n”-shaped narrow passages.

The authors are with the State Key Laboratory for Turbulence and Complex Systems, Department of Mechanics and Engineering Science, College of Engineering, Peking University, Beijing 100871, China (e-mail: zhongkli@pku.edu.cn).

## II. RELATED WORK

### A. Optimization-based Trajectory Planning

In optimization-based multi-robot planners, trajectory planning is formulated as a numerical optimization problem, where the inter-robot collision avoidance is leveraged by adding convex [3], [4] or non-convex [14], [15] constraints. Nonetheless, most of the existing methods encounter a challenge that the optimization may be infeasible under these constraints. To overcome this drawback, the method in [13] adopts a soft constraints instead of a hard one, which however may lead to the result that the safety of planned trajectory cannot be ensured. Other methods [11] solve the feasibility problem where the relative safe corridor is used to guarantee the feasibility. Unfortunately, it computes the trajectories sequentially instead of in a concurrent way, e.g., [3], [16]. This indicates that the robot would waste a large amount of time in waiting for others replanning. Besides the optimization feasibility, another problem in trajectory planning is the deadlock, which refers to the fact that robots will be trapped by each other in collision avoidance [5], [11], [17]. A common solution is the right-hand rule [16] based on an artificial perturbation [8], but the inter-robot collision avoidance cannot be ensured. Our previous work [6] is well performed in deadlock resolution via an adaptive right-hand rule, which however is only applicable in obstacle-free space. In conclusion, feasibility guarantee and deadlock resolution in an obstacle-dense environment is still an open problem for multi-robot trajectory planning.

### B. Safe corridor

An early work related to the safe corridor is [18], which generates the corridor through semi-definite programming. The work [19] produces the safe corridor using two steps, namely, sampling-based path planning and geometry-based corridor construction, and achieves a high-speed replanning for quadrotors. Unfortunately, the constraints introduced by the corridor cannot always be satisfied, which implies the optimization may be infeasible, and the same problem can also be observed in [8], [20]. In addition, the authors in [10], [11], [12] propose a construction method by expanding the rectangular corridor in a grid map. Despite this method is computationally efficient, the constructed corridors are restricted by its rectangular shape that may have a lower space efficiency. The method in [21] generates a safe corridor by using supported vector machine, which has a higher utility rate of space but is centralized and offline. Another way to construct a safe corridor is voxel expansion [8], [9], where a performed corridor is constituted based on a grid map. However, the construction there is achieved offline as well, and cannot handle dynamic missions such as changing targets.

## III. PROBLEM STATEMENT

This section formulates the optimization-based trajectory planning problem in a cluttered environment with dimension  $d = 2, 3$ . The goal is to drive  $N$  robots from their initial positions to respective destinations in an environment with obstacles. During this period, a robot cannot collide with *any*

other robot or *any* obstacle. Despite every robot can only determine its own control input, the information of others can be obtained via wireless communication. The trajectory is replanned and executed every sampling time step and the replanning is reformulated as a numerical optimization with finite variables.

### A. Trajectory Representation

Let  $h$  denote the sampling time step. In the time step  $t$  of replanning, the planned trajectory for robot  $i$  is defined as  $\mathcal{P}^i(t) = [p_1^i(t), p_2^i(t), \dots, p_K^i(t)]$  where  $p_k^i(t)$ ,  $k \in \mathcal{K} := \{1, 2, \dots, K\}$ , is the planned position at time  $t + kh$  and  $K$  is the length of horizon. Similarly, let  $v_k^i(t)$ ,  $k \in \mathcal{K}$  denote the velocity at time  $t + kh$  and let  $u_k^i(t)$ ,  $k = \{0, 1, \dots, K - 1\}$  denote the control input. The dynamics of the robot are formulated as

$$\dot{x}_k^i(t) = \mathbf{A}x_{k-1}^i(t) + \mathbf{B}u_{k-1}^i(t), \quad k \in \mathcal{K}, \quad (1)$$

where  $x_k^i(t) = [p_k^i(t), v_k^i(t)]$  is the planned state at time  $t + kh$ ,  $x_0^i(t) = x^i(t)$  and

$$\mathbf{A} = \begin{bmatrix} \mathbf{I}_d & h\mathbf{I}_d \\ \mathbf{0}_d & \mathbf{I}_d \end{bmatrix}, \quad \mathbf{B} = \begin{bmatrix} \frac{h^2}{2}\mathbf{I}_d \\ h\mathbf{I}_d \end{bmatrix}. \quad (2)$$

Additionally, the velocity and input constraints are given as

$$\|\Theta_a u_{k-1}^i(t)\|_2 \leq a_{\max}, \quad k \in \mathcal{K}, \quad (3)$$

$$\|\Theta_v v_k^i(t)\|_2 \leq v_{\max}, \quad k \in \mathcal{K}, \quad (4)$$

where  $\Theta_v, \Theta_a$  are positive-definite matrices, and  $v_{\max}, a_{\max}$  denote the maximum velocity and acceleration, respectively.

Assume that once the planned trajectory is updated, the lower feedback controller can perfectly track it in the time interval  $[t, t + h]$ . As a result, when replanning at time  $t + h$ , the current state of the robot satisfies  $x^i(t + h) = x_1^i(t)$ . Fortunately, the current tracking controller, e.g. [22], is qualified to fulfill this assumption and is adopted in our hardware experiments.

In cooperative navigation, the information of different robots is exchanged by wireless communication. Moreover, it is assumed that the modified historically planned trajectory is informed and called predetermined trajectory, defined as  $\bar{\mathcal{P}}^i(t) = [\bar{p}_1^i(t), \bar{p}_2^i(t), \dots, \bar{p}_K^i(t)]$ , where  $\bar{p}_k^i(t) = p_{k+1}^i(t - h)$ ,  $k \in \tilde{\mathcal{K}} := 1, 2, \dots, K - 1$  and  $\bar{p}_K^i(t) = p_K^i(t - h)$ .

### B. Collision Avoidance

1) *Inter-robot Collision Avoidance*: To avoid the collision among robots, the minimum distance allowed between any pair of robots is set to be  $r_{\min} > 0$ , implying that a collision happens when  $\|p^i - p^j\|_2 \leq r_{\min}$ <sup>1</sup>. Moreover, the replanned trajectories of robots  $i$  and  $j$  are collision-free if the positions of different pairs of robots are larger than  $r_{\min}$  at not only the sampling time  $t + kh$ ,  $k \in \mathcal{K}$  but also during the interval time.

<sup>1</sup>For the sake of simplicity, the time index  $t$  will be omitted whenever ambiguity is not caused. For example,  $p^i(t)$  will be rewritten as  $p^i$ .

2) *Obstacle Avoidance*: Let  $\mathcal{O}$  denote the collection of obstacles. Then the obstacle avoidance requires that the occupied circle or sphere for a robot in the configuration space should not have contact with any obstacle, i.e.,  $(p^i \oplus r_a \mathbf{I}_d) \cap \mathcal{O} = \emptyset$ , where  $\oplus$  is the Minkowski sum and  $r_a$  is the radius of agents. Furthermore, a planned trajectory  $\mathcal{P}$  is collision-free, if its position is collision-free at not only the sampling time but also during the interval time. Similar to [20], [23], we assume that the obstacles are convex-shaped.

#### IV. TRAJECTORY PLANNING METHOD

The trajectory planning method will be provided in this section. We deal with the inter-robot collision avoidance, deadlock resolution and then obstacle avoidance. Subsequently, the complete trajectory planning method is summarized, followed by the proof for the feasibility guarantee of the proposed method.

##### A. Inter-robot Collision Avoidance

For inter-robot collision avoidance, we introduce the modified buffered Voronoi cell with warning band (MBVC-WB) [6] as depicted in Fig. 2. Define the following parameters:

$$a_k^{ij} = \frac{\bar{p}_k^i - \bar{p}_k^j}{\|\bar{p}_k^i - \bar{p}_k^j\|_2}, \quad b_k^{ij} = a_k^{ijT} \frac{\bar{p}_k^i + \bar{p}_k^j}{2} + \frac{r'_{\min}}{2}, \quad (5)$$

where  $r'_{\min} = \sqrt{r_{\min}^2 + h^2 v_{\max}^2}$  denotes the extended minimum distance. Then, the MBVC-WB can be formulated by

$$a_k^{ijT} p_k^i \geq b_k^{ij}, \quad \forall j \neq i, k \in \tilde{\mathcal{K}}, \quad (6a)$$

$$a_K^{ijT} p_K^i \geq b_K^{ij} + w^{ij}, \quad \forall j \neq i, \quad (6b)$$

where  $w^{ij}$  is an additional variable added to the optimization and satisfies

$$0 \leq w^{ij} \leq \epsilon. \quad (7)$$

In (7),  $\epsilon$  is referred to as the maximum width of warning band.

The additional penalty term added to the cost function is given by

$$C_w^i = \sum_{j \neq i} \frac{1}{\epsilon \gamma^{ij}} \rho_{ij} w^{ij2}, \quad (8)$$

where  $\gamma^{ij}(t) = (1 - \beta) \gamma^{ij}(t - h) + \beta w^{ij}(t - h)$ ,  $\beta \in (0, 1)$  and  $\gamma^{ij}(t_0) = \epsilon$ . Notably, the modified function (8) is a quadratic term and is computationally efficient in the sense that  $\gamma^{ij}(t)$  related to the result of  $w^{ij}$  in last time step  $t - h$  is utilized to adjust the weight of this penalty. Additionally,  $\rho_{ij}$  is an important coefficient designed to execute adaptive the right-hand rule and will be presented later.

##### B. Deadlock Resolution

To deal with the possible deadlock problem in inter-robot collision avoidance, we propose a detection-resolution mechanism. For deadlock detection, a notion of terminal overlap is introduced as follows: If there holds  $p_K^i(t) \neq p_{\text{target}}^i$ ,  $p_K^i(t) = p_K^i(t - h)$ , and  $p_K^i(t) = p_{K-1}^i(t)$ , we say that a terminal overlap happens and it is denoted by  $b_{\text{TO}}^i = \text{True}$ .

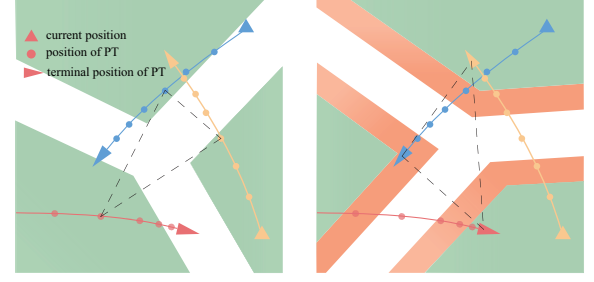


Fig. 2. Illustration of the MBVC-WB where the green area is the feasible space and the orange one is the warning band. Shared space is split at each horizon (Left). In particular, for terminal horizon, warning band is added (Right).

Regarding deadlock resolution, the adaptive right-hand rule is carried out by adjusting  $\rho^{ij}$  as follows

$$\rho^{ij} = \rho_0 e^{\eta^i(t) \sin \theta^{ij}}, \quad (9)$$

where

$$\eta^i(t) = \begin{cases} \eta^i(t - h) + \Delta\eta & \text{if } b_{\text{TO}}^i = \text{True}, \\ 0 & \text{if } w^{ij} = 0, \forall j \neq i, \\ \eta^i(t - h) & \text{else.} \end{cases} \quad (10)$$

In (9) and (10),  $\rho_0 > 0$  and  $\Delta\eta > 0$  are the coefficients; the initial condition of  $\eta^i$  is  $\eta^i(t_0) = 0$ ; the parameter  $\theta^{ij}$  is defined as the angle in  $x - y$  plane between the projection of  $p_K^i$  to  $p_{\text{target}}^i$  and  $p_K^j$  to  $p_K^j$ .

##### C. Obstacle Avoidance

The obstacle avoidance is realized by restricting the planned trajectory in a safe corridor. The corridor is constituted by a sequence of convex polyhedra in which the edge can separate the planned positions  $p_k^i$  and inflated obstacle  $\tilde{\mathcal{O}}$ , i.e., the obstacle inflated by  $r_a$  in (Fig. 3, the blue polygons shifted by green obstacles). In our method, the corridor is formed upon the predetermined trajectory. As an example in Fig. 3(d), three intersected convex polyhedra make up a corridor. Based on the safe corridor, the obstacle avoidance constraint can be written as

$$a_k^{i,oT} p_k^i \geq b_k^{i,o}, \quad (11)$$

where  $a_k^{i,o}$  and  $b_k^{i,o}$  constitute the edge of corridor for robot  $i$  at horizon  $k \in \mathcal{K}$ . In the following subsections, the method of constructing these planes will be clarified in detail.

1) *Path Planning*: To begin with, a path is required to indicate an approximated direction for a robot to the destination. This path is a collision-free polyline that connects the robot and its target, i.e., connecting terminal horizon position of predetermined trajectory,  $\bar{p}_K^i$  and target,  $p_{\text{target}}^i$  as shown in Fig 3(a). RRT\*-based methods are qualified to find such a feasible path, and among these methods, the Advanced Batch Informed Trees (ABIT\*) [7] has a higher path quality. Thus, ABIT\* is utilized to find the path and the length of this path is chosen as objective to be minimized.

Once the path is found, a point  $p_{\text{tractive}}^i$ , called the tractive point, will be chosen in this path. It is determined as the closet point in the path to the target such that the line segment between this point and  $\bar{P}_K^i$  is collision-free. A demo is presented

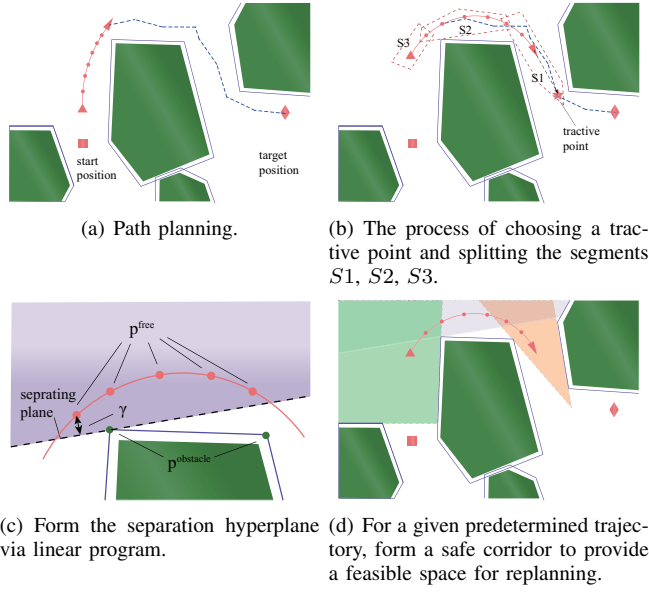


Fig. 3. Process of forming safe corridor.

in Fig. 3(b). Then, if a terminal overlap does not happen, i.e.,  $b_{TO}^i = False$ , we add the tractive point to the end of predetermined trajectory to form the extended predetermined trajectory (EPT). In practice, we find that, in most of situations, a tractive point can be obtained via previously planned path. In other words, the path is unnecessary to be updated in every replanning. Thus, the path planning is triggered when it is needed such as changing the target or failing to find a tractive point.

2) *Segment Division*: After obtaining EPT, we need to divide the points of EPT into several segments so as to decrease the computation requirements as shown in Fig 3(b). Firstly, we choose the end point of EPT as the start of the first segment. Next, from the second end point of EPT to the start, the point in EPT will be added into the current segment one by one. We will stop to add the next point into the current segment until the convex hull of the contained points is not collision-free anymore. Then, a new segment will begin from the end point of the last one. The above process will be repeatedly carried out until the beginning point  $\bar{p}_1^i$  is added into the segment.

3) *Separating Plane*: After diving points of EPT into several segments, we will construct the separating plane between the segment and obstacles. Since the convex hull formed by the points in each segment is obstacle-free and also the obstacles are convex-shaped, a separating plane exists according to separating hyperplane theorem [24]. Then, as shown in Fig 3(c), an optimization-based method can be provided as follows:

$$\begin{aligned}
 & \max_{a,b,\gamma} \gamma, \\
 \text{s.t.}, & \quad a^T p^{\text{free}} \geq \gamma + b, \\
 & \quad a^T p^{\text{obstacle}} \leq b, \\
 & \quad \|a\|_2 = 1, \\
 & \quad \gamma \geq 0,
 \end{aligned} \tag{12}$$

---

**Algorithm 1:** GetCorridor()

---

```

input :  $\mathcal{O}, \bar{\mathcal{P}}^i(t)$ 
output:  $ObCons$ 
1 if Need Path Planning then
2    $Path^i(t) \leftarrow ABIT^*(\bar{p}_K^i, p_{\text{target}}^i, \mathcal{O});$ 
3 else
4    $Path^i(t) \leftarrow Path^i(t - h);$ 
5 end
6  $ObCons \leftarrow \emptyset;$ 
7  $Segmentlist \leftarrow \text{SegmentDivision}(\mathcal{O}, \bar{\mathcal{P}}^i(t), Path^i(t));$ 
8 for  $Segment \in Segmentlist$  do
9    $Corridor \leftarrow \text{GetCorridor}(Segment, \mathcal{O});$ 
10   $ObCons \cup \text{AddConstraints}(Corridor);$ 
11 end

```

---

where  $a$  and  $b$  determine the separating plane;  $p^{\text{free}}$  and  $p^{\text{obstacle}}$  denote the points of segments and obstacles respectively;  $\gamma$  is the margin variable. Such an optimization can be further transformed to the following quadratic program (QP):

$$\begin{aligned}
 & \min_{a',b'} \|a'\|_2^2 \\
 \text{s.t.}, & \quad a'^T p^{\text{free}} \geq 1 + b', \\
 & \quad a'^T p^{\text{obstacle}} \leq b',
 \end{aligned} \tag{13}$$

where  $a' = \frac{a}{\gamma}$  and  $b' = \frac{b}{\gamma}$ . By solving the QP (13), the separating plane can be obtained as  $a = \frac{a'}{\|a'\|_2}$  and  $b = \frac{b'}{\|a'\|_2}$ , which forms the edge of a convex polyhedron. Moreover,  $a_k^{i,o}$  and  $b_k^{i,o}$  are chosen as  $a$  and  $b$ , respectively, to formulate the constraints (11).

In implementation, the separation between segments and obstacles are unnecessary to be constructed in some occasions that the obstacle locates out of the planning region. Therefore, we come up with the following manipulation to simplify the planning process. Specifically, the separating plane will be computed from the nearest obstacle to the farthest one. Regarding each obstacle, a separating plane will be built if this obstacle has a contact with the currently formed convex polyhedra. Otherwise, such an obstacle will be omitted. In addition, if the distance between the obstacle and the robot is larger than  $K h v_{\text{max}}$ , the obstacle will not be considered either.

4) *Safe Corridor Construction*: All above, the algorithm of forming a safe corridor is concluded in Alg. 1, where the detail process has been illustrated sequentially in previous sub-subsections. This safe corridor generation method has some critical properties, which is summarized as follows.

**Lemma 1.** *The safe corridor formulation method provided in Alg. 1 has the following three properties:*

- 1) *If the predetermined trajectory  $\bar{\mathcal{P}}$  is obstacle-free, a safe corridor can be generated.*
- 2) *The underlying predetermined trajectory  $\bar{\mathcal{P}}$  satisfies the formulated constraints (11), i.e.,  $a_k^{i,oT} \bar{p}_k^i \geq b_k^{i,o}$ ,  $k \in \mathcal{K}$ .*
- 3) *If the constraints (11) formulated by the safe corridor are satisfied, the planned trajectory  $\mathcal{P}$  is obstacle-free.*

*Proof.* 1) Based on the above-mentioned method, we can conclude that a division of segment can be found if a predetermined trajectory is obstacle-free. This is because the line between the tractive point and  $\bar{p}_K^i$  is collision-free, which obviously leads to a collision-free EPT. In this case, the worst and most conservative division is all the segments are only formed by the adjacent two points of EPT. Additionally, since there exist separating planes between the points of segment and any of obstacle, the convex polyhedra can be formed. Consequently, the safe corridor can be constituted by a sequence of polyhedra.

2) Since the constraints (11) are obtained from the optimization (12) with  $p^{\text{free}}$  chosen as the positions from predetermined trajectory, it clear that the predetermined trajectory  $\bar{\mathcal{P}}$  satisfies these constraints.

3) As aforementioned, for a collision-free predetermined trajectory, a division of segment can be found. Then, due to the segment division rule, it is obvious that the adjacent points of predetermined trajectory, e.g.,  $\bar{p}_k^i$  and  $\bar{p}_{k+1}^i$ , must be contained in a common segment. Thus, if the constraints is enforced, the corresponding planned points  $p_k^i$  and  $p_{k+1}^i$  must be restricted to a common convex polyhedron. Consequently, the line segment between them must be obstacle-free. Then, regarding a finished segment division, all points of predetermined trajectory are included because the segment division can be completed if and only if the point is counted sequentially until the last one. Thus, all the line segments of the trajectory is covered by a collision-free safe corridor.  $\square$

#### D. Trajectory Planning Algorithm

In the previous subsections, the methods dealing with inter-robot and robot-obstacle collision avoidance are formulated to be certain kinds of constraints into the optimization problem. Furthermore, another constraint is introduced to ensure the feasibility of the underlying optimization, that is,

$$v_K^i = \mathbf{0}_d. \quad (14)$$

Moreover, we enforce that  $x_k^i = x_K^i$ ,  $k > K$  and  $u_k^i = \mathbf{0}_d$ .

In addition to the constraints, the proposed cost function for robot  $i$  is given by

$$C^i = C_p^i + C_w^i, \quad (15)$$

where  $C_w^i$  is provided in (8) and  $C_p^i$  is given by

$$C_p^i = \frac{1}{2} Q_K \|p_K^i - p_{\text{tractive}}^i\|_2^2 + \frac{1}{2} \sum_{k=1}^{K-1} Q_k \|p_{k+1}^i - p_k^i\|_2^2. \quad (16)$$

Note that  $C_p^i$  is employed to drive the robots to the current tractive point and  $Q_k$ ,  $k \in \mathcal{K}$  in (16) is the weight parameter.

Therefore, the optimization can reformulated as follows.

$$\begin{aligned} \min_{u^i, x^i, w^{ij}} \quad & C^i \\ \text{s.t.} \quad & (1), (3), (4), (6), (7), (11), (14). \end{aligned}$$

Based on this optimization, the proposed trajectory planning method is summarized in Algorithm 2. The inputs are the initial position  $p^i(t_0)$ , the target position  $p_{\text{target}}^i$  and obstacles

---

#### Algorithm 2: The Complete Algorithm

---

**Input :**  $p^i(t_0), p_{\text{target}}^i, \mathcal{O}$

```

1  $\bar{\mathcal{P}}^i(t_0) \leftarrow \text{InitialPredTraj}(p^i(t_0))$ ;
2  $b_{\text{TO}}^i \leftarrow \text{False}$ ;
3 while not all robots at target do
4   for  $i \in \mathcal{N}$  concurrently do
5      $\bar{\mathcal{P}}^j(t) \leftarrow \text{Communicate}(\bar{\mathcal{P}}^i(t))$ ;
6      $\text{cons}^i \leftarrow \text{GetInterCons}(\bar{\mathcal{P}}^i(t), \bar{\mathcal{P}}^j(t))$ ;
7      $\text{cons}^i \leftarrow \text{cons}^i \cup \text{GetCorridor}(\mathcal{O}, \bar{\mathcal{P}}^i(t))$ ;
8      $x^i(t) \leftarrow \text{GetCurrentState}()$ ;
9      $\mathcal{P}^i(t), w^{ij} \leftarrow \text{Optimization}(\text{cons}^i, x^i(t))$ ;
10     $b_{\text{TO}}^i \leftarrow \text{DeadlockDetection}(\mathcal{P}^i(t), w^{ij})$ ;
11     $\bar{\mathcal{P}}^i(t+h) \leftarrow \text{GetPredTraj}(\mathcal{P}^i(t))$ ;
12    ExecuteTrajectory( $\mathcal{P}^i(t)$ );
13  end
14   $t \leftarrow t+h$ ;
15 end
```

---

$\mathcal{O}$ . To begin with, the predetermined trajectory is initialized as  $\bar{\mathcal{P}}^i(t_0) = [p^i(t_0), \dots, p^i(t_0)]$  and  $b_{\text{TO}}^i$  is set as False. After this initialization, in the main loop, each robot run their respective algorithm in parallel (Line 4). At the beginning, the predetermined trajectory is informed among the robots (Line 5), followed by the procedure that the functions related to inter-robot and robot-obstacle collision avoidance are realized (Line 6-7). After obtaining the current state, the optimization (17) is formulated and resolved (Line 9). Afterwards, the deadlock detection is made (Line 10) based on the resolution of the optimization and the predetermined trajectory in next step is derived thereafter (Line 11). Finally, the planned trajectory is executed (Line 12).

#### E. Feasibility Guarantee

Different from most existing optimization-based methods, the proposed planner guarantees the feasibility of the optimization problem, which is illustrated in the following theorem.

**Theorem 1.** *If the initial positions of all robots are collision-free, the robots will never have collisions with each other or any obstacles.*

*Proof.* At beginning time  $t_0$ , the predetermined trajectory is initialized as  $\bar{\mathcal{P}}^i(t_0) = [p^i(t_0), \dots, p^i(t_0)]$ . Choosing it as the planned trajectory, i.e.,  $p_k^i(t_0) = \bar{p}_k^i(t_0)$ , it is naturally that this planned trajectory satisfies all constraints listed in optimization (17). Thus, at time  $t_0$ , the optimization is feasible for all robots.

Thereafter, we intend to prove that our algorithm is recursively feasible, i.e., once the optimization at time step  $t-h$  are feasible, we can find a feasible solution at time  $t$ . Form Lemma 1, we already know that if planned trajectory at  $t-h$  is feasible, it must be obstacle-free and we can find a safe corridor in this time's replanning. Afterwards, the final optimization (17) can be formulated. Given feasible solution at last time step,  $u_{k-1}^i(t-h)$  and  $x_k^i(t-h)$  for  $k \in \mathcal{K}$ , we can provide a



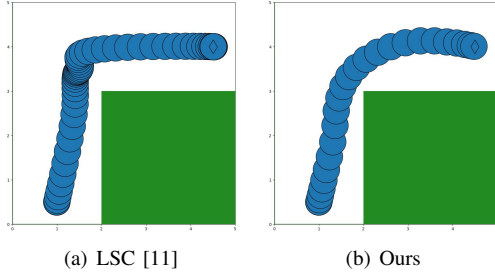


Fig. 4. The scenario 'L'-passage for LSC [11] and ours.

feasible solution  $x_k^i(t) = x_{k+1}^i(t-h)$ ,  $u_k^i(t) = u_{k+1}^i(t-h)$  and  $w^{ij}(t) = \min\{\epsilon, a_K^{ijT}(t)p_K^i(t) - b_K^{ij}(t)\}$ , where we enforce that  $x_K^i(t) = x_{K+1}^i(t-h) = x_K^i(t-h)$  and  $u_K^i(t) = u_e$ .

First, as the result of optimization at time step  $t-h$ ,  $x_{k+1}^i(t-h)$  and  $u_{k+1}^i(t-h)$  with  $k \in \tilde{\mathcal{K}}$ , satisfy the constraints in (1), (3)-(4) naturally. In addition, since  $x_K^i(t) = x_{K+1}^i(t-h) = x_K^i(t-h)$  and  $u_{K-1}^i(t) = u_K^i(t-h) = u_e$  hold,  $x_K^i(t)$  and  $u_{K-1}^i(t)$  also satisfy these constraints. In the meantime, as  $x_K^i(t) = x_{K+1}^i(t-h) = x_K^i(t-h) = x_{K-1}^i(t)$  holds, it is evident that the constraint (14) holds as well. Then, towards constraints related to MBVC-WB, i.e., (6), (7), the feasibility of the provided solution have been proved in our previous work [6]. Lastly, regarding constraint (11), as property 1) and 3) stated in Lemma 1, for given feasible solution in time  $t-h$ , the previously planned trajectory is obstacle-free and a formulation of safe corridor can be found at this time. Afterwards, according to property 3), the provided solution, i.e., the predetermined trajectory, satisfies these constraints evidently. Thus, the constraint (11) is feasible and the optimization is feasible in a recursive way.

Since the initial optimizations as well as thees successive ones are feasible, the included constraints are satisfied. According to property 3) in Lemma 1 and the property of MBVC-WB in [6], the obstacle and inter-robot collision can be avoided.  $\square$

## V. NUMERICAL SIMULATIONS AND EXPERIMENTS

In this section, we will analyze the validation and performance of the proposed algorithm via numerical simulations and hardware experiments. The algorithm is implemented in an Intel Core i9 @3.2GHz computer with Python3 programming language and publicly available at <https://github.com/PKU-MACDLab/IMPC-OB>. We use CVXOPT [25] for quadratic programming and trajectory optimization, and OMPL [26] for ABIT\* path planning. Furthermore, comparisons with Ego-swarm [13], MADER [14] and LSC [11] are carried out.

### A. Numerical Simulations and Comparison

The main parameters of robots are chosen as follows: the minimum inter-agent distance  $r_{\min} = 0.6\text{m}$ ; the radius of agents  $r_a = 0.3\text{m}$ ; the maximum acceleration  $a_{\min} = 2\text{m/s}^2$ ; the maximum velocity  $v_{\max} = 3\text{m/s}$ .

To begin with, we will provide a single robot simulation to show the proposed safe corridor, where the environment is a "L"-passage. Fig. 4 shows the comparative simulation results

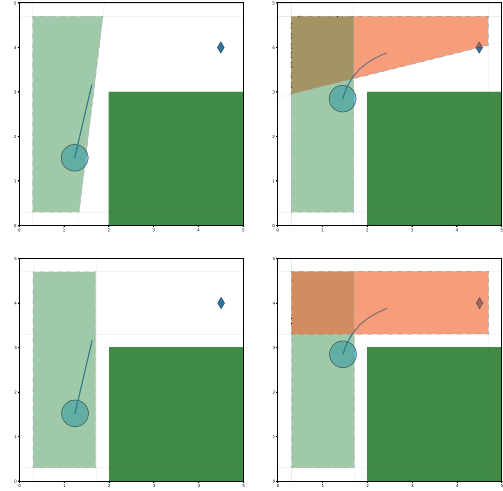


Fig. 5. The generated corridor for given pre-planned trajectory (**Top**: LSC [11] and **Bottom**: Ours ). Noticeably, the provided corridor is the feasible space for the centroid of the robot.

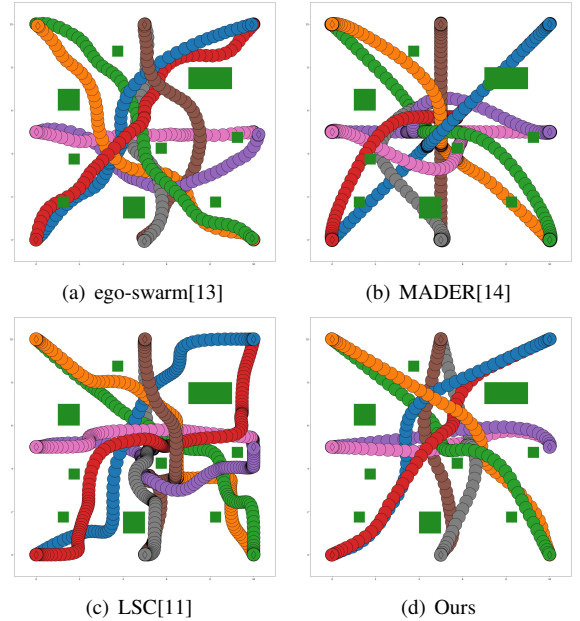


Fig. 6. Four planners are performed in the forest scenario.

of the method proposed in [11] and our method. Notably, our method has a higher speed and smoother trajectory in the sense that our planner cost  $4.1\text{s}$  in comparison with  $7.5\text{s}$  for LSC. The difference between the safe corridors are given in Fig. 5. Compared with the rectangle corridor in LSC, our corridor is a trapezoid, which provides more feasible space for upcoming turning.

Furthermore, comparisons with Ego-swarm, MADER and LSC are made throughout forest-transition and "H"-transition. Trajectories of these scenarios are illustrated in Fig. 6 and Fig. 7, respectively. The results are shown in Table I. For computation time, the proposed method has a relatively long computation time since it is programmed by Python3 that cannot take full advantage of multi-core computation. But in prospective execution, the computation can be carried

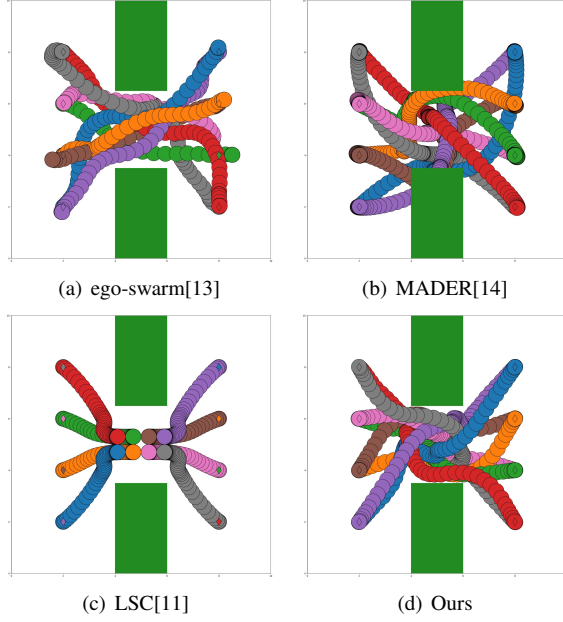


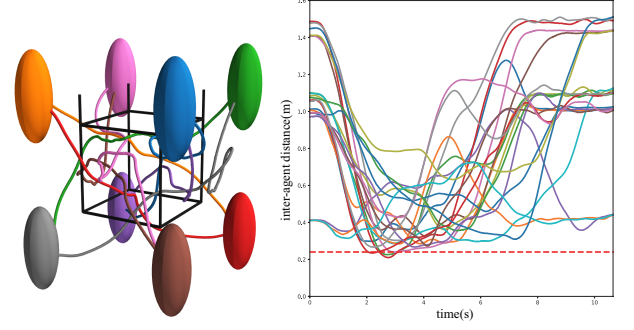
Fig. 7. Four planners are performed in the “H” scenario.

TABLE I

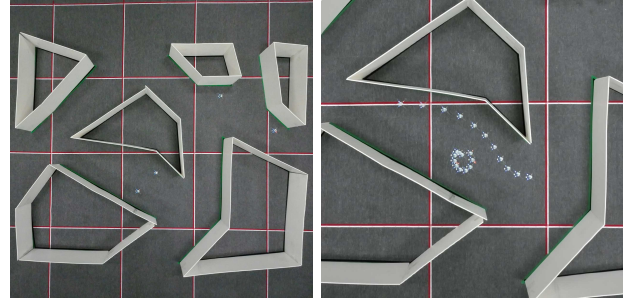
COMPARISON WITH STATE-OF-ARTS. (SAFETY: NO COLLISION OCCURS.  $T_t$ [s]: TRANSITION TIME.  $L_t$ [m]: THE LENGTH OF TRANSITION.  $T_c$ [ms]: MEAN COMPUTATION TIME PER REPLANNING.)

|        | method         | Safety | $T_t$ | $L_t$  | $T_c$ |
|--------|----------------|--------|-------|--------|-------|
| forest | Ego-swarm [13] | No     | 9.2   | 105.8  | 9.6   |
|        | MADER [14]     | No     | 22.3  | 111.1  | 104.0 |
|        | LSC [11]       | Yes    | 22.3  | 114.34 | 53.2  |
|        | Ours           | Yes    | 8.1   | 102.4  | 93.0  |
| “H”    | Ego-swarm [13] | No     | 7.5   | 66.6   | 10.2  |
|        | MADER [14]     | No     | 14.2  | 71.5   | 116.7 |
|        | LSC [11]       | Yes    | -     | -      | 62.3  |
|        | Ours           | Yes    | 9.3   | 67.7   | 86.8  |

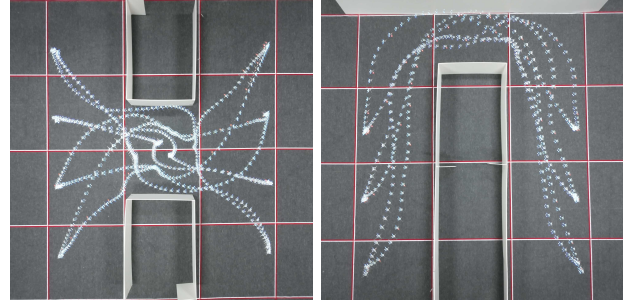
out in multiple processors concurrently, and the time will decrease considerably. Ego-swarm has an impressive computation time in addition to a relative smooth and fast trajectories. Unfortunately, it cannot guarantee the collision avoidance, since it adopts an unconstrained optimization in planning. For MADER, the optimization under the strict constraints guarantees the avoidance between robots. However, regarding obstacle-avoidance, MADER seems to be maladaptive in an obstacle-dense environment as several collision appears. LSC has the feasibility guarantee which ensures the safety of robots, but a deadlock occurs in “H”-transition. Despite heuristic deadlock resolution method is adopted in LSC, it is ineffective in this scenario. Though we similarly utilize linear constraint to handle inter-agent collision, the extra warning band introduce an elastic interaction instead of a hard one, based on which, the adaptive right-hand rule is leveraged, resulting in right-hand rotations in the bottleneck of the “H”. Moreover, for transition time and length, the proposed planner has a considerable superiority which means a faster and smoother trajectories.



(a) **Left:** the trajectories of this swarm where the ellipsoids indicate the minimum inter-robot distance. **Right:** the distances between different pairs of robots.



(b) **left:** four crazyfiles are deployed in a polyhedron-shape environment. **Right:** When a crazyfile go through the narrow passage, another quadrotor make a way to let it pass by.



(c) **Left:** The hardware experiment of “H”-transition. **Right:** “n”-transition.

Fig. 8. The real-world experiments.

### B. Hardware Experiments

Hardware experiments are executed on the platform of crazyswarm [27], where multiple nano-quadrotors are flying under a motion capture system OptiTrack. The computation of all robots is done on a central computer with frequency, 5Hz to comply with the sampling time step  $h = 0.2s$ . For each crazyfile, a feedback controller [22] is adopted to track the planned trajectory.

The first experiment is shown in Fig. 8(a), where 8 crazyfiles fly through a 0.6m cubic framework. Considering the air turbulence, a crazyfile in the inter-robot avoidance is represented as an ellipsoid with diameter 0.24m in the  $x - y$  plane and 0.6m in the  $z$  axis. Owing to the deformation of robots, the inter-robot constraints are accordingly adjusted by modifying  $a_k^{ij}$  and  $b_k^{ij}$  as

$$a_k^{ij} = E \frac{E(\bar{p}_k^i - \bar{p}_k^j)}{\|E(\bar{p}_k^i - \bar{p}_k^j)\|_2}, \quad b_k^{ij} = a_k^{ij} \frac{E(\bar{p}_k^i + \bar{p}_k^j)}{2} + \frac{r'_{\min}}{2},$$

where  $E = \text{diag}(1.0, 1.0, \frac{0.24}{0.6})$ ;  $r'_{\min} = \sqrt{r_{\min}^2 + v_{\max}^2}$  and  $r_{\min} = 0.24\text{m}$ . The radius of a crazyfile is set as  $r_a = 0.12\text{m}$ . From the result given in Fig 8(a), it is apparent that the crazyfiles can achieve this transition.

In addition, four crazyfiles moving in a cluttered environment are shown in Fig 8(b). Given initial positions, the targets are randomly chosen. After arriving at the targets, the new one will be published immediately and this process is repeated 5 times. In this scenario, the feasible space is the irregular-shaped passage at the interval of polygon-shaped obstacles where the width of these passages ranges from 0.4m to 0.7m. By the help of MBVC-WB, where the warning band introduces an elastic interaction between the robots, a robot can squeeze out a way between the wall and other robots to avoid this trap as shown in Fig. 8(b). Such an inter-robot coordination in this scenario solves the deadlock problem.

At last, other two experiments as illustrated in Fig. 8(c) are carried out, where the scenarios are “H”-transition and “n”-transition, respectively. In these navigations, the safety is guaranteed and the coordination in narrow passage is properly achieved. In “H”-transition, the right-hand rotation appears as in the previous simulation. Regarding the “n”-transition, the intersection of two groups of quadrotors at the top passage is the main challenge for this mission. It can be seen that the proposed method resolves it as the quadrotors fly through the passage without sacrificing any speed. For a quadrotor, when encountering an oncoming agent, it can rapidly find a side to avoid collisions by utilizing MBVC-WB.

## VI. CONCLUSION

This work has proposed a novel multi-robot trajectory planning method for obstacle-dense environments wherein the collision avoidance is guaranteed and the deadlock among robots is resolved. In contrast to state-of-the-art works, the proposed method’s performance of safety and deadlock resolution in cluttered scenarios can be ensured by theoretical proof and validated by comprehensive simulations and hardware experiments.

## REFERENCES

- [1] S.-J. Chung, A. A. Paranjape, P. Dames, S. Shen, and V. Kumar, “A survey on aerial swarm robotics,” *IEEE Transactions on Robotics*, vol. 34, no. 4, pp. 837–855, 2018.
- [2] X. Zhou, X. Wen, Z. Wang, Y. Gao, H. Li, Q. Wang, T. Yang, H. Lu, Y. Cao, C. Xu, and F. Gao, “Swarm of micro flying robots in the wild,” *Science Robotics*, vol. 7, no. 66, p. eabm5954, 2022.
- [3] L. C. E. and A. P. Schoellig, “Trajectory generation for multiagent point-to-point transitions via distributed model predictive control,” *IEEE Robotics and Automation Letters*, vol. 4, no. 2, pp. 375–382, 2019.
- [4] F. Augugliaro, A. P. Schoellig, and R. D’Andrea, “Generation of collision-free trajectories for a quadcopter fleet: A sequential convex programming approach,” in *2012 IEEE/RSJ International Conference on Intelligent Robots and Systems (IROS)*, 2012, pp. 1917–1922.
- [5] J. Alonso-Mora, P. Beardsley, and R. Siegwart, “Cooperative collision avoidance for nonholonomic robots,” *IEEE Transactions on Robotics*, vol. 34, no. 2, pp. 404–420, 2018.
- [6] Y. Chen, M. Guo, and Z. Li, “Deadlock resolution and recursive feasibility in mpc-based multi-robot trajectory generation,” *arXiv preprint arXiv:2202.06071*, 2022.
- [7] M. P. Strub and J. D. Gammell, “Advanced BIT (ABIT): Sampling-based planning with advanced graph-search techniques,” in *2020 IEEE International Conference on Robotics and Automation (ICRA)*, 2020, pp. 130–136.
- [8] C. Toumeh and A. Lambert, “Decentralized multi-agent planning using model predictive control and time-aware safe corridors,” *IEEE Robotics and Automation Letters*, vol. 7, no. 4, pp. 11 110–11 117, 2022.
- [9] F. Gao, L. Wang, B. Zhou, X. Zhou, J. Pan, and S. Shen, “Teach-repeat-replan: A complete and robust system for aggressive flight in complex environments,” *IEEE Transactions on Robotics*, vol. 36, no. 5, pp. 1526–1545, 2020.
- [10] J. Park, J. Kim, I. Jang, and H. J. Kim, “Efficient multi-agent trajectory planning with feasibility guarantee using relative bernstein polynomial,” in *2020 IEEE International Conference on Robotics and Automation (ICRA)*, 2020, pp. 434–440.
- [11] J. Park, D. Kim, G. C. Kim, D. Oh, and H. J. Kim, “Online distributed trajectory planning for quadrotor swarm with feasibility guarantee using linear safe corridor,” *IEEE Robotics and Automation Letters*, vol. 7, no. 2, pp. 4869–4876, 2022.
- [12] J. Li, M. Ran, and L. Xie, “Efficient trajectory planning for multiple non-holonomic mobile robots via prioritized trajectory optimization,” *IEEE Robotics and Automation Letters*, vol. 6, no. 2, pp. 405–412, 2021.
- [13] X. Zhou, J. Zhu, H. Zhou, C. Xu, and F. Gao, “Ego-swarm: A fully autonomous and decentralized quadrotor swarm system in cluttered environments,” in *2021 IEEE International Conference on Robotics and Automation (ICRA)*, 2021, pp. 4101–4107.
- [14] J. Tordesillas and J. P. How, “Mader: Trajectory planner in multiagent and dynamic environments,” *IEEE Transactions on Robotics*, pp. 1–14, 2021.
- [15] M. Kamel, J. Alonso-Mora, R. Siegwart, and J. Nieto, “Robust collision avoidance for multiple micro aerial vehicles using nonlinear model predictive control,” in *2017 IEEE/RSJ International Conference on Intelligent Robots and Systems (IROS)*, 2017, pp. 236–243.
- [16] D. Zhou, Z. Wang, S. Bandyopadhyay, and M. Schwager, “Fast, on-line collision avoidance for dynamic vehicles using buffered Voronoi cells,” *IEEE Robotics and Automation Letters*, vol. 2, no. 2, pp. 1047–1054, 2017.
- [17] L. Wang, A. D. Ames, and M. Egerstedt, “Safety barrier certificates for collisions-free multirobot systems,” *IEEE Transactions on Robotics*, vol. 33, no. 3, pp. 661–674, 2017.
- [18] R. Deits and R. Tedrake, *Computing Large Convex Regions of Obstacle-Free Space Through Semidefinite Programming*. Springer International Publishing, 2015, pp. 109–124.
- [19] S. Liu, M. Watterson, K. Mohta, K. Sun, S. Bhattacharya, C. J. Taylor, and V. Kumar, “Planning dynamically feasible trajectories for quadrotors using safe flight corridors in 3-D complex environments,” *IEEE Robotics and Automation Letters*, vol. 2, no. 3, pp. 1688–1695, 2017.
- [20] B. Şenbaşlar, W. Hönig, and N. Ayanian, “Rlss: Real-time multi-robot trajectory replanning using linear spatial separations,” *arXiv preprint arXiv:2103.07588*, 2021.
- [21] W. Hönig, J. A. Preiss, T. K. S. Kumar, G. S. Sukhatme, and N. Ayanian, “Trajectory planning for quadrotor swarms,” *IEEE Transactions on Robotics*, vol. 34, no. 4, pp. 856–869, 2018.
- [22] D. Mellinger and V. Kumar, “Minimum snap trajectory generation and control for quadrotors,” in *2011 IEEE International Conference on Robotics and Automation (ICRA)*, 2011, pp. 2520–2525.
- [23] X. Ma, Z. Jiao, Z. Wang, and D. Panagou, “Decentralized prioritized motion planning for multiple autonomous uavs in 3d polygonal obstacle environments,” in *2016 International Conference on Unmanned Aircraft Systems (ICUAS)*, 2016, pp. 292–300.
- [24] S. Boyd, S. P. Boyd, and L. Vandenberghe, *Convex optimization*. Cambridge university press, 2004.
- [25] A. Martin, D. Joachim, and V. Lieven, “Cvxopt,” Website, <http://cvxopt.org/>.
- [26] I. A. Şucan, M. Moll, and L. E. Kavraki, “The Open Motion Planning Library,” *IEEE Robotics & Automation Magazine*, vol. 19, no. 4, pp. 72–82, December 2012, <https://ompl.kavrakilab.org>.
- [27] J. A. Preiss, W. Hönig, G. S. Sukhatme, and N. Ayanian, “Crazyswarm: A large nano-quadcopter swarm,” in *2017 IEEE International Conference on Robotics and Automation (ICRA)*, 2017, pp. 3299–3304.